

Phenomenology of Electron Solvation in Polar Fluids

Peter Graf and Abraham Nitzan*

School of Chemistry, Tel Aviv University, Tel Aviv 69978, Israel

Geerd H. F. Diercksen

MPI für Astrophysik, Karl-Schwarzschild-Str.1, Postfach 1523, D-85740 Garching, Germany

Received: April 2, 1996; In Final Form: September 6, 1996[⊗]

The phenomenology of electron solvation in polar solvents is studied by investigating the characteristics of electron solvation in a model polar solvent, a Stockmayer liquid characterized by a combination of Lennard-Jones and dipolar intermolecular interactions which interacts with the electron with a combination of short range repulsive and of electrostatic (dipole–charge) interactions. Energetics and dynamical properties of the solvated electron are studied as functions of the solvent density and of solvent molecular parameters which determine the electron solvent interaction and the solvent dynamical response. We find that electron localization in this solvent is caused primarily by the repulsive part of the electron–solvent interaction. Upon increasing the solvent molecular dipole from zero, the electron becomes more localized; however, this effect seems to saturate at moderate solvent polarities, and further increase of the polarity changes the ground (and excited) state energies without affecting strongly the electron size. In this regime the electron behaves approximately like a classical charge distribution as far as the dependence of its solvation energy on the solvent polarity is concerned. The dynamical response of the solvent to the solvated electron is investigated by studying the solvent-induced fluctuations of the electron's energy levels. As expected we find that fluctuations in the ground and excited state energies are dominated by the electrostatic part of the electron–solvent interaction, and their dynamics therefore reflects the solvent rotational motion. Surprisingly, however, the electrostatic contributions mostly cancel in the fluctuations of the gap between the ground and first excited state. Consequently the gap fluctuations are dominated by the solvent translational motions. The implications of these observations on the dynamics of electron solvation are discussed.

1. Introduction

Recent studies of solvation dynamics in polar liquids may be divided into two categories. On one hand, intensive work has been carried out in order to elucidate the nature of the solvent dynamical response to a sudden change (usually induced by an optical transition) in the solute charge distribution.¹ Theoretical studies of such processes have assumed that the process is classical in nature: the dynamics of charge rearrangement in the solute (itself a quantum process) is assumed to be instantaneous on the observable time scale, and the consequent solvent motion is treated using classical mechanics and electrostatics. The underlying assumption (confirmed by numerical simulations) is that solvent intramolecular vibrations (for which classical mechanics is questionable at room temperature) do not play an important role in the solvation process. Theoretical studies and numerical simulations of such processes have yielded important information about the nature of solvation dynamics in simple polar solvents. In particular, the existence of an important inertial ultrafast component in the solvation processes was discovered,^{1,2} and the predominance of solvent rotational and librational motions has been established.^{1,3,4}

On the other hand, electron solvation has also been the focus of a considerable amount of recent work. In a typical experiment the formation of the solvated electron following electron injection into, e.g., water is monitored.⁵ Such experiments together with numerical simulations have established that an important route to the formation of the fully solvated electron involves as a rate-determining step the *nonadiabatic* transition from the lowest excited (“p-like”) to the ground (“s-like”) state

of the solvated electron in its already formed solvent cavity.^{5–7} The process is thus essentially quantum mechanical. The same nonadiabatic transition can be probed directly by monitoring the relaxation following photoexcitation of the solvated electron.⁸

While the nature of the solvent motions which dominate solvation dynamics in polar solvents has been addressed in several studies,^{1–3} this issue has not been explicitly raised with respect to electron solvation. It is first important to distinguish between adiabatic solvation (processes which occur on a single electronic state) and nonadiabatic relaxation as described above. Adiabatic solvation can be generated in computer simulations by confining the electron to a single electronic state throughout the relaxation, but the corresponding dynamics is an important ingredient also of the nonadiabatic relaxation, since it determines the fluctuations of the energy gaps between the electronic states. Barnett et al.⁹ have pointed out that the short time component of the *adiabatic* hydration dynamics of an electron is sensitive to H–D substitution, indicating that librational motions of the water hydrogens as well as H-bond dynamics dominate this part of the solvation. In fact, this process is very similar to the classical dynamics which takes place following the sudden generation of an anion of size similar to the final size of the hydrated electron (~ 2 Å). More detailed studies have been carried out by Rossky and co-workers.¹⁰ In particular Schwartz and Rossky^{10a} have recently performed numerical simulations of electron hydration dynamics in the ground state as well as in the excited (p-like) state manifold of the hydrated electron, using a flexible SPC water model together with an electron water pseudopotential developed by Schnitker and Rossky.¹¹ They have concluded that low-frequency translational motions of the

[⊗] Abstract published in *Advance ACS Abstracts*, November 1, 1996.

solvent play an important role in both the inertial and the diffusive portions of the relaxation. This observation is related to the fact that unlike in the solvation process which follows the instantaneous change in the charge distribution of classical solutes, much of the local change in the solvation structure about a solvating electron is associated with a significant change in size and shape of the electron upon change in its quantum state. Another important observation is that for this system the solvent linear response function

$$C(t) = \frac{\langle \delta U(0) \delta U(t) \rangle}{\langle (\delta U)^2 \rangle} \quad (1)$$

where $U(t)$ is the value of the quantum energy gap at time t and $\delta U(t) = U(t) - \langle U \rangle$ represents the fluctuation of the gap from its equilibrium average value, provides a good approximation to the nonequilibrium response function

$$S(t) = \frac{\langle U(t) \rangle_{\text{ne}} - \langle U(\infty) \rangle_{\text{ne}}}{\langle U(0) \rangle_{\text{ne}} - \langle U(\infty) \rangle_{\text{ne}}} \quad (2)$$

where the $\langle \rangle_{\text{ne}}$ denotes a nonequilibrium ensemble average.

The importance of solvent translational modes in electron hydration dynamics has been highlighted by a recent suggestion by Rips¹² that the rate-determining step in the formation of the ground state solvated electron is not the nonadiabatic $p \rightarrow s$ transition but the compression of the cavity toward its final size. Rips has shown that, assuming that water is essentially incompressible, the time scale associated with this process is comparable to that observed experimentally. Furthermore, the dominance of water *translational* motion explains in this model the observed smallness of H–D isotope effect on the relaxation rate.^{5b,4f,8} Rips' simplistic picture is not confirmed by numerical simulations; however, it also emphasizes the role of solvent translations as an important ingredient in the electron solvation process. Furthermore, solvent translations associated with the formation of the solvation cavity (e.g. the "electron bubble" in liquid He¹³) are expected to constitute a major ingredient in electron solvation processes in nonpolar fluids.

From the point of view of general methodology, electrons provide a unique probe in solvation dynamics studies for three reasons: First, the nonadiabatic nature of the actual solvation process as discussed above provides an important example of a solvation process dominated by quantum mechanical effects. Secondly, the considerable shape and size changes associated with the electron dynamics constitute another unique ingredient in this solvation process. Finally, the charge distribution changes in a way different from that of most probes: upon s to p excitation this change would correspond to the sudden formation of a quadrupole if these states were of exact s and p characters. This is another factor which enhances the importance of solvent translational modes in this solvation process because of the relative short range of the interaction.

The rate of a nonadiabatic transition between two electronic states in condensed phases is closely related to the dynamics of the *adiabatic* fluctuations of the energy gap between the two states. For example, a simple semiclassical perturbative expression for the nonadiabatic rate in terms of the gap fluctuations is given by^{14,15}

$$k_{\text{NA}} = \frac{|V_{\text{NA}}|^2}{\hbar^2} \int_{-\infty}^{\infty} \langle \exp[i \int_0^{\tau} \omega(t) dt] \rangle_{\text{T}} d\tau \quad (3a)$$

where V_{NA} is the nonadiabatic coupling between the two electronic states, $\hbar\omega$ is the fluctuating energy gap, and $\langle \rangle_{\text{T}}$

denotes thermal averaging. In eq 3 the noncommutativity between the electronic potential operators evaluated at different times was disregarded. A second-order cumulant expansion (exact if $\omega(t)$ is a Gaussian stochastic process) can then be used to express k_{NA} in terms of the gap correlation function $C(t)$, leading to^{14,15}

$$k_{\text{NA}} = \frac{|V_{\text{NA}}|^2}{\hbar^2} \exp[iM_1(t) - M_2(t)] \quad (3b)$$

$$M_1(t) = \int_0^t dt' \langle \omega(t') \rangle$$

$$M_2(t) = \int_0^t dt' \int_0^{t'} dt'' [\langle \omega(t'') \omega(t') \rangle - \langle \omega(t'') \rangle \langle \omega(t') \rangle]$$

Neria and Nitzan⁶ have pointed out that in addition to the gap fluctuations, the quantum nature of the solvent may contribute by affecting the Franck–Condon factor associated with the transition. Very recently, Schwartz et al.^{10c} have invoked this idea to explain the apparent lack of H–D isotope effect on the $p \rightarrow s$ relaxation of the hydrated electron.^{5,8} Still, the gap fluctuations are the dominant factor affecting the overall rate of the nonadiabatic process, and understanding the way they are influenced by different solvent motions is therefore of central importance in understanding the solvent effect on the electron solvation process.

In this paper we investigate numerically the effect of a classical solvent on a quantum solute, focusing on the interplay between the short range repulsive and the long range electrostatic electron–solvent interactions and on the relative roles played by solvent translational and rotation/librational modes. Since we emphasize generic issues we use a generic model solvent: a Stockmayer solvent (Lennard-Jones spheres with point dipoles in their centers) whose mass and moment of inertia are chosen independently. Comparing results obtained for different sets of these solvent parameters, we can determine the relative importance of solvent rotational and translational motions in the relaxation processes that determine electron solvation.

2. Technical Details

Our solvent is a generic Stockmayer solvent, characterized by intermolecular Lennard-Jones plus dipole–dipole interactions. These interactions are determined by three parameters: the Lennard-Jones energy and length parameters, ϵ and σ , and the molecular dipole μ . In addition, the solvent dynamical properties depend on its molecular mass M and moment of inertia I , which are varied independently in the present study, as well as on the density ρ and temperature T . A typical simulated system consists of 100 such classical particles at $T = 240$ K, in a cubic box of size 39.52 au (corresponding to 1.09×10^{22} particles/cm³, the density of MeCl at this temperature) with reaction field boundary conditions.¹⁶ For the electron–solvent interaction we also take a generic form: a sum of electrostatic interaction and short range repulsive terms. The former is determined by the electron charge and the solvent dipole. The latter is taken, following Zhu and Cukier,²² to be of the form

$$V^{(s)} = A \exp\left[-\left(\frac{r}{l}\right)^6\right] \quad (4)$$

Detailed forms of all interaction terms including those imposed by the reaction field boundary conditions, together with the proper cutoffs imposed by the chosen system size, are provided in Appendix A.

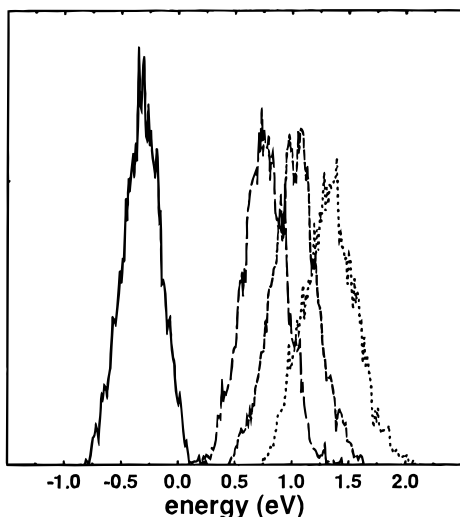


Figure 1. Distributions of the ground and the three lowest excited states energies of the solvated electron in a Stockmayer solvent with MeCl parameters. Data are obtained from a 100 ps ground state trajectory.

In what follows, unless otherwise stated, atomic units are used for energy, length, and charge, and $(1/12)$ carbon-mass is taken as the mass unit. Correspondingly, the time unit is $[m^2/E]^{1/2} = 1.033 \times 10^{-15}$ s. The classical time evolution is carried out using the velocity Verlet algorithm, with a time step $\Delta t \leq 1.14$. Our starting model parameters correspond to the methyl chloride (MeCl) solvent, with molecular mass and dipole moment $M = 50$ and $\mu = 0.7357$, respectively, and LJ parameters $\epsilon = 6.175 \times 10^{-4}$ and $\sigma = 7.937$. The constraint on the magnitude of the molecular dipole (see ref 3) is kept using the Rattle algorithm.¹⁷ Temperature control is achieved by imposing thermal collisions on the solvent particles (Andersen's method¹⁸). The quantum propagation is carried out within the adiabatic simulation scheme:¹⁹ the electron is restricted to a particular quantum state throughout the evolution. The electronic wave function is defined on a 16^3 grid, with grid spacing 2.0625. With this choice we obviously restrict ourselves to states which are well localized inside the grid. The exterior dielectric constant used for the reaction field boundary condition is determined self-consistently by computing the dielectric response of the simulated sample. For the MeCl solvent $\epsilon' = 17$. The quantum states and energies are obtained using an iterative block-Lanczos method, using FFT in the calculation of the Hamiltonian operation. The calculation of average energies (and, in principle, spectra) is achieved by obtaining the electronic energy levels (and dipole matrix elements) for an ensemble of equilibrium system configurations. Adiabatic time evolution on the i th electronic state is carried out by propagating the classical solvent under the potential $V_{\text{sol-sol}} + \langle \Psi_i | V_{\text{el-sol}} | \Psi_i \rangle$, re-evaluating the state Ψ_i at each classical step according to the instantaneous solvent configuration.

As a starting point for the following numerical investigation we take the Stockmayer solvent with methyl chloride parameters, in which classical solvation dynamics has been extensively studied. The short range electron solvent interaction parameters are taken to be $A = 1$ au and $l = \sigma/2$. The equilibrium distributions of the ground and the three lowest excited states energies of the electron in this solvent are shown in Figure 1. The ground state distribution peaks at ~ -0.35 eV and has a width of ~ 0.25 eV. The excited states associated with the ground state cavity have positive energies, in the range 0.3–1.8 eV. In the following sections we examine the effect of changing the character of the electron–solvent interaction on

TABLE 1: Dependence of the Ground State Energy, E_g , Ground State Gyration Radius, R_g , and the First Electronic Energy Gap on Some Solvent Parameters^a

μ	ρ	σ	E_g (eV)	R_g (eV)	ΔE (eV)
0	1.0	1.0	1.19	3.28	0.81
1.0	1.0	1.0	-0.33	2.87	1.09
1.4	1.0	1.0	-0.64	2.87	1.10
1.0	0.9	1.0	-0.33	3.12	0.91
1.0	1.1	1.0	-0.31	2.68	1.27
1.0	1.0	0.97	-0.38	3.01	0.98
1.0	1.0	1.03	-0.28	2.73	1.21

^a The solvent molecular dipole moment μ , its density ρ , and its LJ diameter σ are given relative to the corresponding values of MeCl (see text).

the electron binding to the solvent and on the electronic energy levels and the effect of changing solvent mass and moment of inertia (i.e. changing the characteristics of the solvent translational and rotational motions) on the dynamics of electron solvation.

3. Energetics

Previous numerical investigations of the solvated electron have focused on particular solvent models such as water, ammonia, simple hydrocarbons, and rare gases. The ground state properties of the solvated electron and the associated solvent structure have been investigated for models of these fluids using numerical simulations as well as theoretical treatments based on the RISM-polaron theory²⁰ and on the mean field approximation.^{21,22} Our generic model contains the main characteristics of a polar solvent in which the electron experiences a combination of short range repulsive and of electrostatic interactions and can be continuously transformed into a nonpolar solvent by taking the molecular dipole μ to be zero. Here we examine the effect of the electron–solvent interaction on the energetic characteristics and on the localization properties of the solvated electron. In particular we focus on the average ground state energy E_g and localization radius $R_g = [\langle \Psi_g | r^2 | \Psi_g \rangle - \langle \Psi_g | r | \Psi_g \rangle^2]^{1/2}$ and on the energy gap between the ground and first excited state. Table 1 shows the effect on these quantities of changing the dipole moment μ , the density ρ , and the diameter σ of the solvent molecules. Note that σ also determines the short range electron solvent interaction (4) by $l = \sigma/2$. It is seen that a moderate change in the polar fluid density makes a relatively small change on the total electronic energies. This, however, results from the compensating effect of changing the magnitudes of both the (positive) kinetic energy and the (negative) potential energy components. The ground state energy as well as the ground state gyration radius are very sensitive to the solvent molecular dipole. This dependence is strong for small μ and seems to saturate at some transition value μ_t (see Figure 2). For $\mu > \mu_t$ the electron's wave function (and R_g) becomes relatively independent of μ , and the main effect of changing μ is associated with the classical response of a given charge distribution to a changing electrostatic field.²³ For this reason the magnitude of the electronic energy gap hardly changes, while the ground state energy changes by a factor of ~ 2 when μ changes from the MeCl value (0.736) to the water value (1.03). It should be added that increasing the molecular dipole of the pure solvent from $\mu = 0$ to the MeCl value causes a reduction in pressure in the simulated constant volume system. For our MeCl model this would amount to increasing the density by ~ 5 –10% if the pressure was to be kept constant. Therefore the effect on the electron's energy levels of increasing the solvent molecular dipole from zero *at constant pressure* is expected to be considerably larger than for the corresponding constant volume system.

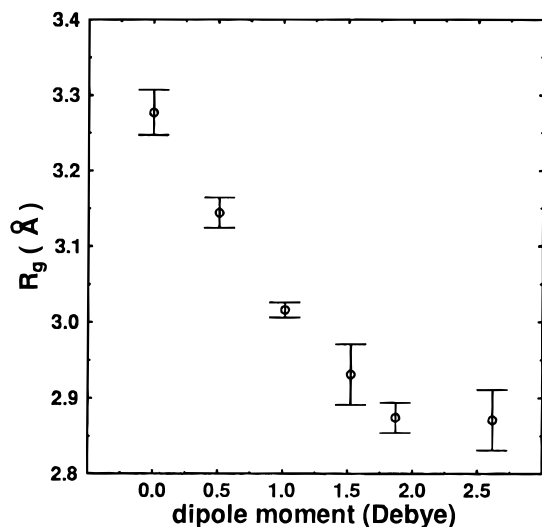


Figure 2. Localization radius, radius $R_g = [\langle \Psi_g | r^2 | \Psi_g \rangle - \langle \Psi_g | r | \Psi_g \rangle^2]^{1/2}$, of the solvated electron as a function of solvent polarity expressed in terms of its molecular dipole moment. The error bars reflect the accuracy of the calculation based on averages calculated from five independent trajectories.

These results are consistent with the observations of Zhu and Cukier,²² who have noted that even for strong polar solvents like water the electron remains localized (with a localization size of the same order) when the electrostatic interactions are switched off. In fact, the mean field calculation by these authors shows almost no effect of the electrostatic forces on the ground state size; however, numerical results based on the SPC water model shows a stronger effect (13% increase in R_g upon switching off the electrostatic interactions), comparable to the results of the present Stockmayer model. In any case these calculations show the crucial role played by the short range repulsive forces in determining the structure of the solvated electron.

Finally, the electronic energies seem to be quite sensitive to the molecular diameter σ . This is probably a consequence of the fact that when the nearest electron–solvent distance decreases, the electrostatic attraction which shifts the electronic energies downward becomes more prominent.

4. Dynamics of Levels and Gap Fluctuations

While adiabatic simulations restrict the electron to a single quantum level, the information obtained from such simulations can be used to calculate nonadiabatic transition rates in the small electron–solvent coupling. Here we study the effect of different solvent motions on these dynamical fluctuations. At issue is the relative importance of solvent translational and rotational degrees of freedom.²⁴ Starting from the MeCl parameters $M = 50$ and $I = 119.8$ we have studied the effect of changing M and I on the dynamics of the solvent-induced fluctuations in the electronic energy levels, on the energy gap between the ground and the first excited state, and on the size (estimated by the gyration radius) of the solvated electron. Table 2 summarizes the different sets of parameters used in these calculations.

The ratio p provides an estimate of the relative importance of rotational and translational motions in the solvent dynamics. The effects of these different choices of parameter sets on the pure solvent dynamics are shown in Figures 3 and 4. Figure 3 shows the normalized time correlation functions of the solvent velocity, $C_v(t) = \langle \mathbf{v}(0) \cdot \mathbf{v}(t) \rangle / \langle v^2 \rangle$, and the angular velocity, $C_w(t) = \langle \mathbf{w}(0) \cdot \mathbf{w}(t) \rangle / \langle w^2 \rangle$ ($\mathbf{w} = \dot{\boldsymbol{\mu}}$), and also of the dipole

TABLE 2: Parameter Sets Used in the Simulations of Dynamical Response^a

case	M	I	$p = I/(2M\sigma^2)$
M1	261.7	119.8	0.0036
“MeCl”	50	119.8	0.019
M2	3.80	119.8	0.25
I1	50	22.7	0.0036
I2	50	1574.9	0.25

^a “MeCl” denotes the parameter set associated with the Stockmayer model of methyl chloride. M1 and M2 are similar sets with different solvent mass. I1 and I2 are similar sets with different solvent moment of inertia.

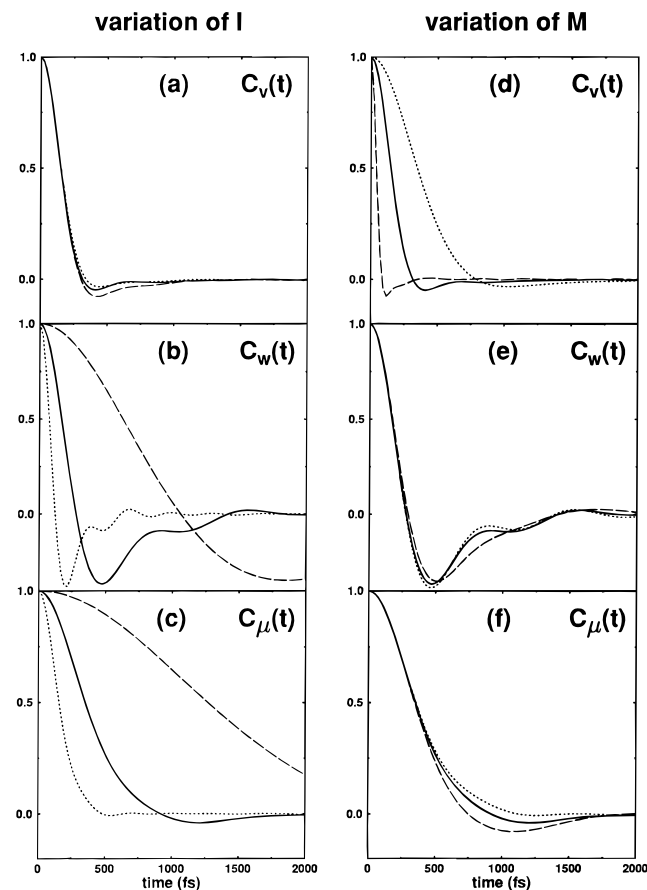


Figure 3. Time correlation functions of the pure solvents: (a) and (d) center of mass velocity correlation function $C_v(t)$; (b) and (e) angular velocity correlation function, $C_w(t)$; (c) and (f) orientation correlation function, $C_\mu(t)$. In a–c $M = 50$ and the molecular moment of inertia is changed; dashed line, full line, and dotted line correspond to $I = 1574.9, 119.8,$ and 22.7 , respectively. In d–f $I = 119.8$ and the solvent molecular mass is varied, and dashed, full and dotted lines correspond to $M = 3.80, 50,$ and 261.7 , respectively. Note that the full lines correspond to the “standard” MeCl parameters. Therefore the full lines in the corresponding left and right figures are identical.

orientation $C_\mu(t) = \langle \boldsymbol{\mu}(0) \cdot \boldsymbol{\mu}(t) \rangle / \mu^2$. Figure 4 shows the Fourier transforms, $C(\omega) = \int_{-\infty}^{\infty} dt \cos(\omega t) C(t)$, of the velocity and angular velocity correlation functions. Obviously, increasing M suppresses the translational contributions, while increasing I suppresses the rotational contributions to the solvent dynamics.

Figures 5 show the normalized time correlation functions for ground state energy fluctuations. Also given are the averages $\langle E \rangle$ and the standard deviations $\langle \delta E^2 \rangle^{1/2}$ of the different components of the electronic energy. Note that these numbers should not depend on M and I . Shown are the correlation functions for the total electronic energy, together with its potential and kinetic energy components. The following observations can be made: (a) The fluctuations in the total

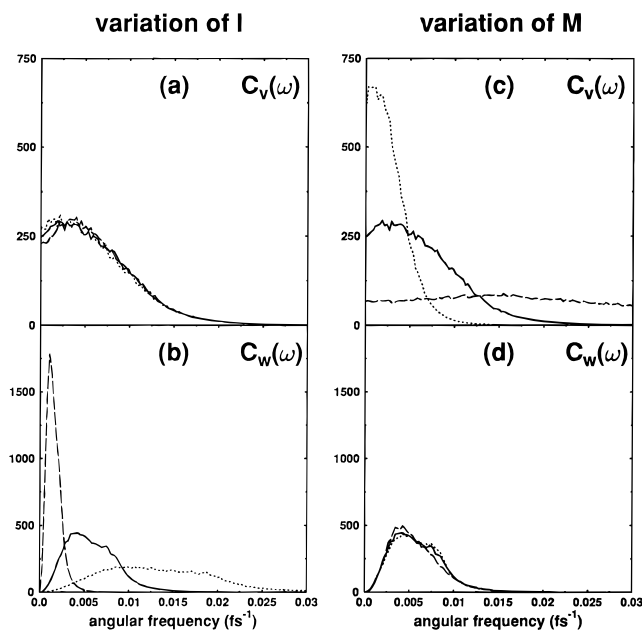


Figure 4. Fourier transforms of the velocity and angular velocity correlation functions shown in Figure 3. Line notation is the same as in Figure 3.

ground state energy are much more sensitive to the solvent moment of inertia than to its mass (compare parts a and f of Figure 5), indicating that solvent rotations are dominant in this dynamics. (b) The kinetic energy fluctuations show the expected sensitivity to the solvent mass (Figure 5j), i.e. to the solvent translations. (c) The *short range* part of the potential energy behaves very similarly to the kinetic energy (Figure 5i,j); however, the long range electrostatic part of the potential energy dominates the total energy fluctuations, which are therefore nearly insensitive to the solvent mass. Comparing parts d, e and i, j of Figure 5 shows the strong correlation between the kinetic energy and the short range potential energy fluctuations. The strong correlation between these quantities can be realized also by computing cross correlations such as $\langle \delta E_{\text{kin}} \delta V_{\text{short}} \rangle / [\langle \delta E_{\text{kin}}^2 \rangle \langle \delta V_{\text{short}}^2 \rangle]^{1/2}$ (this yields 0.95, 0.92, 0.90, and 0.88 for the four lowest states of the solvated electron). A similar picture is obtained if instead of fluctuations in the electron kinetic energy we take the electron gyration radius as a measure of its size. Similarly, parts b, c and g, h of Figure 5 show that the potential energy fluctuations are dominated by the long range electrostatic component. The qualitative picture that emerges from these observations is as follows: The short range part of the electron–solvent interaction acts via solvent translational modes as a source for fluctuations in the cavity size. Such fluctuations correspond to high correlation between the kinetic and the short range contribution to the potential energy. The total energy fluctuations are dominated by the substantially larger long range electrostatic part of the electron–solvent potential, which is sensitive mainly to solvent rotations and affects the potential energy without strongly influencing the kinetic energy. As will be seen below, this component of the solvent-induced electronic potential energy affects all energy levels of the lower lying states in an approximately similar way, and its contribution to the gap energy difference is therefore small.

It is interesting to compare this picture with the processes that occur in the classical counterpart of the present system. This classical counterpart may be obtained by replacing the electronic charge distribution by a frozen distribution (which corresponds to one instantaneous solvent configuration) and then treating the electron as a classical particle that interacts with

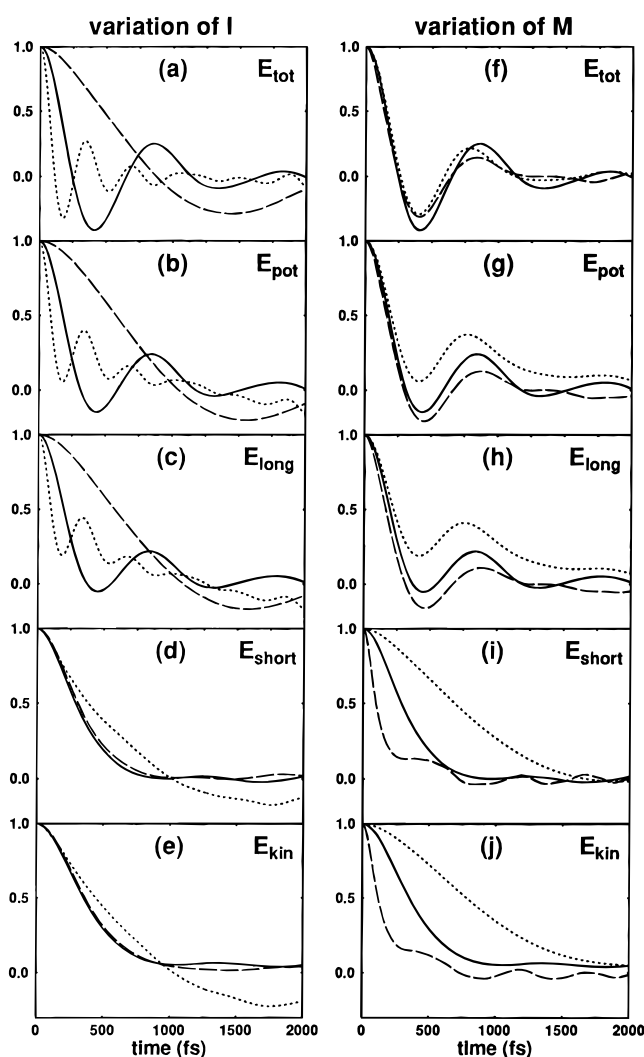


Figure 5. Time correlation functions of the ground state energy fluctuations, for the total energy E_{tot} , the potential energy E_{pot} and its long (E_{long}) and short (E_{short}) range components, and the kinetic energy E_{kin} . Line notations are as in Figures 3 and 4. The averages and the standard deviations of the displayed quantities are (in eV): $E_{\text{tot}} = (-0.33, 0.17)$, $E_{\text{pot}} = (-1.59, 0.20)$, $E_{\text{long}} = (-1.82, 0.21)$, $E_{\text{short}} = (0.22, 0.031)$ and $E_{\text{kin}} = (1.27, 0.095)$, where the first number is $\langle E \rangle$ and the second number is $\langle \delta E^2 \rangle^{1/2}$.

the solvent via the same short range interaction and the electrostatic force associated with this frozen charge distribution. Obviously no kinetic energy fluctuations associated with cavity size exist in this model which is similar to those used to study classical solvation. Figure 6 shows the corresponding time correlation functions. We note that *the total energy fluctuations in this classical system are very similar to those in the quantum case, even though the different components of the potential energy appear different* (compare Figures 5 and 6).

This behavior can be understood from first-order perturbation theory: Let the electronic Hamiltonian be $H = H_0 + \delta V$ where δV denotes the fluctuations in the potential associated with the solvent motion. Let Ψ_0 be an eigenfunction of H_0 corresponding to the energy E_0 , $H_0 \Psi_0 = E_0 \Psi_0$, and $\Psi = \Psi_0 + \delta \Psi$ be an eigenfunction of H with the eigenvalue E , $H \Psi = E \Psi$, where $E = E_0 + \delta E$. Now compare the energy of this system to the energy of a system where the electron behaves as a classical particle whose interaction with the solvent is determined by the frozen distribution $|\Psi_0|^2$, assuming that in either case the solvent motion is the same (i.e. δV is the same; deviations from this assumption appear only in higher than first order in perturbation theory). To first order the fluctuation δE in the total energy is

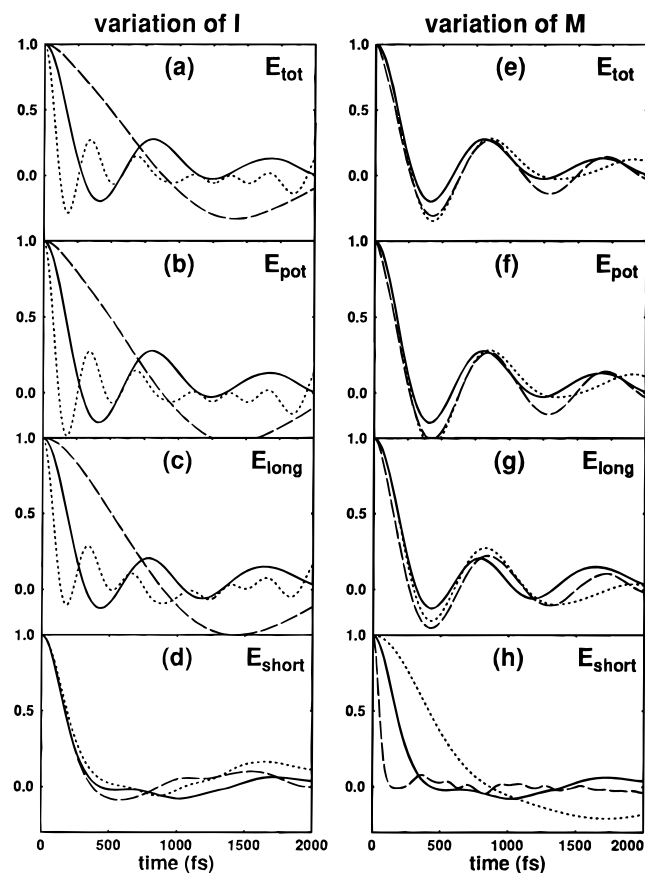


Figure 6. Same as in Figure 5 for the case where the electron's charge distribution is held fixed and invariable under the solvent time evolution. Line notation are as in Figures 3–5.

given to be $\delta E = \langle \Psi_0 | \delta V | \Psi_0 \rangle$, the same in both cases. The kinetic energy component in this fluctuation is, however, zero in the classical (frozen electron distribution) case and different from zero in the quantum case. For example, suppose that the electron–solvent interaction can be modeled as a sum $V = V_1 + V_2$ of a position independent term V_1 and a cavity term V_2 of the form $V_2 = \frac{1}{2}m_e\omega^2r^2$. The thermal motion of the solvent results in a fluctuating V , $\delta V = \delta V_1 + \delta V_2$. Suppose that the fluctuation δV_2 results only from a change in the cavity curvature ω , so that the cavity remains harmonic. For this model $\delta E = \langle \Psi_0 | \delta V_1 + \delta V_2 | \Psi_0 \rangle$ (to first order); however, in the quantum case $\delta E_{\text{pot}} = \langle \Psi_0 | \delta V_1 + \frac{1}{2}\delta V_2 | \Psi_0 \rangle$ and $\delta E_{\text{kin}} = \langle \Psi_0 | \frac{1}{2}\delta V_2 | \Psi_0 \rangle$, while in the classical (frozen) case $\delta E_{\text{pot}} = \langle \Psi_0 | \delta V_1 + \delta V_2 | \Psi_0 \rangle$ and $\delta E_{\text{kin}} = 0$.

The fact that δE is the same in the classical case and (within first-order perturbation theory) in the quantum case, together with the apparent success of linear response theory for this system, is consistent with the observation that the *adiabatic* solvation dynamics of an electron is very similar to that computed for a classical anion of comparable size.²⁵

The observations concerning the relative importance of solvent translational and rotational modes largely repeat themselves when the adiabatic motion on the excited states is considered. However, the fluctuations in the electronic energy gap behave in a *qualitatively* different way. In Figure 7 the normalized time correlation functions for the fluctuations of the 0–1 energy gap (between the ground and the first excited levels of the solvated electron) are displayed. Clearly the gap fluctuations are much more sensitive to the solvent mass than to the solvent moment of inertia, indicating that the solvent *translational* modes are dominant in the variations of this quantity. At the same time these fluctuations are largely

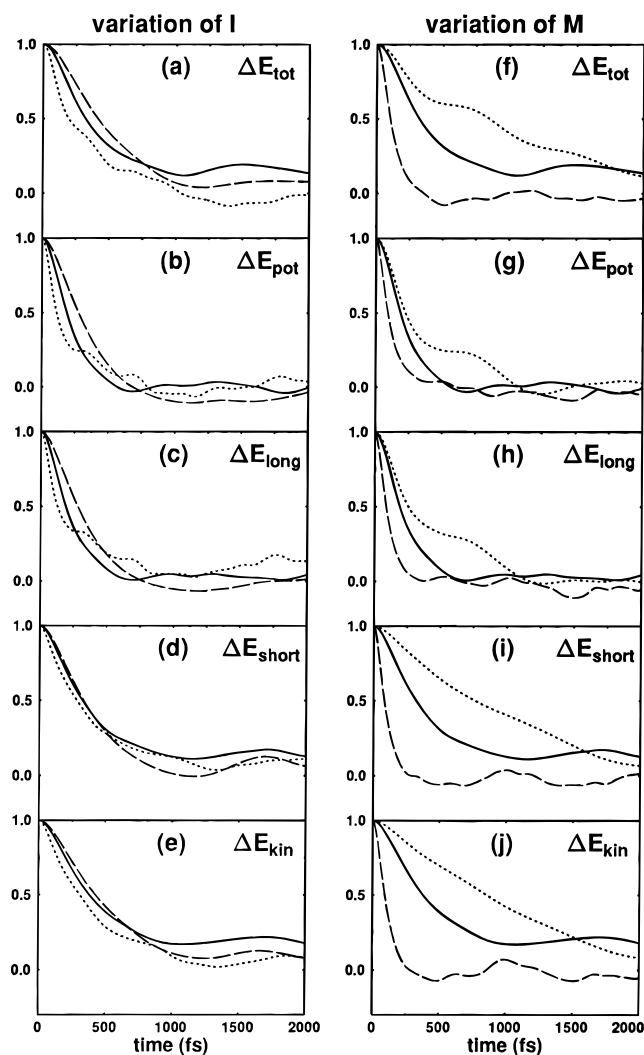


Figure 7. Time correlation functions for the 0–1 energy gap and its different components. Line notations are as in Figures 3–6. The averages and the standard deviations of the displayed quantities are (in eV): $\Delta E_{\text{tot}} = (1.09, 0.12)$, $\Delta E_{\text{pot}} = (0.28, 0.063)$, $\Delta E_{\text{long}} = (0.16, 0.073)$, $\Delta E_{\text{short}} = (0.12, 0.037)$, and $\Delta E_{\text{kin}} = (0.81, 0.11)$, where the first number is $\langle \Delta E \rangle$ and the second number is $\langle \delta(\Delta E)^2 \rangle^{1/2}$.

dominated by the *short* range part of the electron–solvent interaction. A similar pattern is seen in the fluctuations of the 0–2 and 0–3 gaps. It should be noted that an important contribution to this observation is the fact that the solute charge as well as its average dipole moment is the same for all states considered. This makes the relatively short range quadrupole moment of the distribution $|\Psi_s|^2 - |\Psi_p|^2$ the main source of electrostatic energy contribution to the gap fluctuations. It should be also noted that the dominance of the short range part of the electron–solvent interaction in the gap fluctuations implies that dielectric continuum theories (which take into account only the electrostatic interactions) cannot be applicable to the dynamical response.

To summarize, we have observed that the fluctuations of electron's energy levels are largely dominated by its long range electrostatic interaction with the solvent; therefore, the dynamics of these fluctuations is largely controlled by the solvent rotational and librational motions. On the other hand the 0–1 electronic energy gap (as well as the 0–2 and 0–3 gaps) is more sensitive to the short range part of the electron–solvent system, and consequently its dynamics is dominated by the solvent translational motion. For a classical particle with a frozen charge distribution taken from an instantaneous electron

wave function, the total energy fluctuations are very similar to that associated with a quantum electron even though the individual kinetic and potential energy differences are quite different in the two cases.

5. Implications for Electron Solvation Dynamics

The fluctuations in the individual electronic energy levels and fluctuations in the gaps between them are relevant to different physical observables. For example, fluctuations in the ground state energy are associated (within linear response theory) with the dynamics of *adiabatic* solvation on the ground state potential surface, while, as implied by eq 3, fluctuations in the energy gap between two states affect the nonadiabatic transition between these states. If these were the only relevant quantities, we could deduce from the above observations that adiabatic solvation in simple solvents is strongly sensitive to the solvent moment of inertia I (e.g. to the hydrogen mass when water is the solvent) while nonadiabatic solvation is more sensitive to the overall molecular mass.

In fact, there are two additional factors affecting the dependence of the nonadiabatic transition on the molecular moment of inertia, i.e. to the individual masses of the atomic constituents of the molecular solvent: First, the nonadiabatic coupling V_{NA} depends on the angular and linear nuclear velocities of these atomic constituents, and therefore on their masses, and secondly, the solvent contribution to the Franck–Condon factor also depends on the nuclear masses (which affect the tails of the vibrational and librational wave functions). Schwartz et al.^{10c} have argued that a near cancellation of these two effects for the p–s transition of the hydrated electron is the source for the near insensitivity of this process to hydrogen isotopic substitution. It is important to note that there are in fact two cancellation effects: one between the correlated fluctuations of the ground and excited states of the solvated electron which makes the gap fluctuations weakly dependent on the solvent moment of inertia and another between the solvent nuclear mass dependence of the nonadiabatic coupling and between the solvent contribution to the Franck–Condon factor as discussed in ref 10c. It should also be noted that the almost complete cancellation of these dependencies in the case of the p → s transition of the hydrated electron is accidental, and similar processes in other solvents may show a bigger hydrogen isotope effect.

6. Conclusions

We have investigated electron solvation and the dynamics of the electron’s energy level fluctuations in a simple model solvent, as functions of several solvent parameters. For the solvation process, a transition from a quantum localization process to a largely classical electrostatic stabilization is observed as the solvent polarity is increased from zero. The dynamics of energy level fluctuations reveals an interesting interplay between solvent rotational and translational modes. Individual level fluctuations are dominated by solvent rotational and librational motions and are therefore sensitive to the solvent molecular moment of inertia. These effects nearly cancel in the fluctuations of energy *differences* (electronic energy gaps), making these gap fluctuations more sensitive to solvent translations, i.e. to solvent molecular mass. We have argued that this is one of the factors that makes the nonadiabatic p → s relaxation of the hydrated electron nearly insensitive to hydrogen isotope substitution.

Acknowledgment. This research was supported in part by the Israel Science foundation and by the U.S.A.-Israel binational

science foundation. P.G. is thankful to the Minerva-Stiftung for a postdoctoral fellowship. A.N. thanks the Alexander von Humboldt-Stiftung for an Humboldt research award that has made possible his stay in Germany and the MPI für Astrophysik for hospitality during the period when this work was done.

Appendix A. Interaction Potentials

(a) Intermolecular Interaction. The intermolecular Stockmayer potential (V^{STM}), together with the boundary conditions used in our simulations, is given by the sum of a Lennard-Jones potential with spherical cut off (V^{LJ}) and a dipole–dipole potential with tapered reaction field boundary condition (V^{DD})

$$V^{STM}(\mathbf{R}_{ij}, \boldsymbol{\mu}_i, \boldsymbol{\mu}_j) = V^{LJ}(R_{ij}) + V^{DD}(\mathbf{R}_{ij}, \boldsymbol{\mu}_i, \boldsymbol{\mu}_j) \quad (A1)$$

with

$$V^{LJ}(R_{ij}) = 4\epsilon \left[\left(\frac{\sigma}{R_{ij}} \right)^{12} - \left(\frac{\sigma}{R_{ij}} \right)^6 \right] \theta(R_c - R_{ij}) \quad (A2)$$

$$V^{DD}(\mathbf{R}_{ij}, \boldsymbol{\mu}_i, \boldsymbol{\mu}_j) = \left[\left(\frac{1}{R_{ij}^3} - \frac{2(\epsilon' - 1)}{(2\epsilon' + 1)R_{eff}^3} \right) (\boldsymbol{\mu}_i \boldsymbol{\mu}_j) - \frac{3(\mathbf{R}_{ij} \boldsymbol{\mu}_i)(\mathbf{R}_{ij} \boldsymbol{\mu}_j)}{R_{ij}^5} \right] \tau \left(\frac{R_c - R_{ij}}{R_c - R_s} \right) \quad (A3)$$

and

$$\theta(\chi) = \begin{cases} 1 & 0 \leq \chi \\ 0 & \chi < 0 \end{cases} \quad (A4)$$

$$\tau(\chi) = \begin{cases} 1 & 1 \leq \chi \\ \chi & 0 < \chi < 1 \\ 0 & \chi \leq 0 \end{cases} \quad (A5)$$

where \mathbf{R}_i are the positions of classical particles, $\boldsymbol{\mu}_i$ are their dipole moment vectors, and ϵ and σ are the Lennard-Jones potential parameters. R_c is the inner system radius and ϵ' is the exterior dielectric constant used for the reaction field boundary condition. R_{eff} and R_s are parameters used for tapering the cut off in the long range dipole–dipole interaction. Finally, $\mathbf{R}_{ij} = \mathbf{R}_i - \mathbf{R}_j$ and $R_{ij} = |\mathbf{R}_{ij}|$.

For all cases the maximum value for the spherical cut off radius was chosen, i.e. $R_c = L/2$ with L denoting the cubic box length. For the chosen linear tapering function (see ref 16), the effective spherical cut off radius of the reaction field boundary condition is given by

$$R_{eff}^3 = R_s^3 + \frac{3}{R_c - R_s} \left(\frac{R_c^4}{12} + \frac{R_s^4}{4} - \frac{R_c R_s^3}{3} \right) \quad (A6)$$

The onset radius for tapering the electrostatic interactions was chosen, following ref 16, according to $R_s = 0.95R_c$.

(b) Electron Solvent Interaction. The effective potential ($V^{e,S}$) for the interaction of an electron with a classical solvent particle was taken, following ref 22, as a sum of a short range repulsive potential with spherical cut off ($V^{(s)}$) and a switched long range charge–dipole potential with tapered reaction field boundary condition ($V^{(l)}$)

$$V^{e,S}(\mathbf{r}_{ej}, \boldsymbol{\mu}_j) = V^{(s)}(r_{ej}) + V^{(l)}(\mathbf{r}_{ej}, \boldsymbol{\mu}_j) \quad (A7)$$

with

$$V^{(s)}(r_{ej}) = A \exp \left[- \left(\frac{r_{ej}}{l} \right)^6 \right] \theta(R_c - r_{ej}) \quad (A8)$$

$$V^{(1)}(\mathbf{r}_{ej}, \boldsymbol{\mu}_j) = q_e \left(\frac{1}{r_{ej}^1} - \frac{2(\epsilon' - 1)}{(2\epsilon' + 1)R_{\text{eff}}^3} \right) (\mathbf{r}_{ej} \boldsymbol{\mu}_j) f \left(\frac{r_{ej}}{l} \right) \tau \left(\frac{R_c - r_{ej}}{R_c - R_s} \right) \quad (\text{A9})$$

and

$$f(\chi) = 1 - \exp[-\chi^6] \quad (\text{A10})$$

where \mathbf{r}_e is the position of the electron. A and l are the amplitude and the range of the repulsive part of the electron solvent interaction. q_e is the charge of the electron. As before, $\mathbf{r}_{ej} = \mathbf{r}_e - \mathbf{R}_j$ and $r_{ej} = |\mathbf{r}_{ej}|$.

For all cases the range of the repulsive potential was chosen according to $l = \sigma/2$, where σ is the corresponding Lennard-Jones parameter.

References and Notes

- (1) For a review, see: Maroncelli, M. *J. Mol. Liq.* **1993**, *57*, 1. For more recent literature, see refs cited in: Horng, M. L.; Gardecki, J.; Papazyan, A.; Maroncelli, M. *J. Phys. Chem.* **1995**, *99*, 17311. Olender, R.; Nitzan, A. *J. Chem. Phys.* **1995**, *102*, 7180.
- (2) Cho, M.; Rosenthal, S. J.; Scherer, N. F.; Ziegler, L. D.; Fleming, G. R. *J. Chem. Phys.* **1992**, *96*, 5033. Jimenez, R.; Fleming, G. R.; Kumar, P. V.; Maroncelli, M. *Nature (London)* **1994**, *369*, 471. Fee, R. S.; Maroncelli, M. *Chem. Phys.* **1994**, *183*, 235.
- (3) Neria, E.; Nitzan, A. *J. Chem. Phys.* **1992**, *96*, 5433.
- (4) Perera, L.; Berkowitz, M. L. *J. Chem. Phys.* **1992**, *96*, 3092.
- (5) (a) Migus, A.; Gauduel, Y.; Martin, J. L.; Antonetti, A. *Phys. Rev. Lett.* **1987**, *58*, 1559. (b) Gaudel, Y.; Pommeret, S.; Migus, A.; Antonetti, A. *J. Phys. Chem.* **1991**, *95*, 533. (c) Pommeret, S.; Antonetti, A.; Gaudel, Y. *J. Am. Chem. Soc.* **1991**, *113*, 9105. (d) Long, F. H.; Lu, H.; Eienthal, K. B. *Phys. Rev. Lett.* **1990**, *64*, 1469. (e) Long, F. H.; Lu, H.; Shi, X.; Eienthal, K. B. *Chem. Phys. Lett.* **1991**, *185*, 27. (f) Long, F. H.; Lu, H.; Eienthal, K. B. *Chem. Phys. Lett.* **1989**, *160*, 464.
- (6) (a) Neria, E.; Nitzan, A.; Barnett, R. N.; Landman, U. *Phys. Rev. Lett.* **1991**, *67*, 1011. (b) Neria, E.; Nitzan, A. *J. Chem. Phys.* **1993**, *99*, 1109.

- (7) (a) Webster, F. J.; Schnitker, J.; Friedrich, M. S.; Friesner, R. A.; Rossky, P. J. *Phys. Rev. Lett.* **1991**, *66*, 3172. (b) Webster, F. J.; Rossky, P. J.; Friesner, R. A. *Comput. Phys. Comm.* **1991**, *63*, 494.
- (8) Alfano, J. C.; Walhout, P. K.; Kimura, Y.; Barbara, P. F. *J. Chem. Phys.* **1993**, *98*, 5996. Kimura, Y.; Alfano, J. C.; Walhout, P. K.; Barbara, P. F. *J. Phys. Chem.* **1994**, *98*, 3450. Reid, P. J.; Silva, C.; Walhout, P. K.; Barbara, P. F. *Chem. Phys. Lett.* **1994**, *228*, 658.
- (9) Barnett, R. N.; Landman, U.; Nitzan, A. *J. Chem. Phys.* **1989**, *90*, 4413.
- (10) (a) Schwartz, B. J.; Rossky, P. J. *J. Chem. Phys.* **1994**, *101*, 6902. (b) Bittner, E. R.; Rossky, P. J. *J. Chem. Phys.* **1995**, *103*, 8130. (c) Schwartz, B. J.; Bittner, E. R.; Prezhdo, O. V.; Rossky, P. J. *J. Chem. Phys.* **1996**, *104*, 5942.
- (11) Schnitker, J.; Rossky, P. J. *J. Chem. Phys.* **1987**, *86*, 3462.
- (12) Rips, I. *Chem. Phys. Lett.* **1995**, *245*, 79.
- (13) Rosenblit, M.; Jortner, J. *Phys. Rev. Lett.* **1995**, *75*, 4079.
- (14) Lax, M. *J. Chem. Phys.* **1952**, *20*, 1752.
- (15) (a) Warshel, A. *J. Phys. Chem.* **1982**, *86*, 2218. Warshel, A.; Parson, W. W. *Annu. Rev. Phys. Chem.* **1991**, *42*, 279. (b) Sparpaglion, M.; Mukamel, S. *J. Phys. Chem.* **1987**, *91*, 3838; *J. Chem. Phys.* **1988**, *88*, 3263, 4300. Jan; Mukamel. *J. Chem. Phys.* **1988**, *88*, 5735. (c) Borgis, D.; Hynes, J. T. *J. Chem. Phys.* **1991**, *94*, 3619.
- (16) Adams, D. J.; Adams, E. H.; Hills, G. J. *Mol. Phys.* **1979**, *38*, 931.
- (17) Andersen, H. C. *J. Comput. Phys.* **1983**, *52*, 24.
- (18) Andersen, H. C. *J. Chem. Phys.* **1980**, *72*, 2384.
- (19) See, e.g.: Barnett, R. N.; Landman, U.; Nitzan, A. *J. Chem. Phys.* **1988**, *89*, 2242.
- (20) Chandler, D.; Singh, Y.; Richardson, D. M. *J. Chem. Phys.* **1984**, *81*, 1975. Shaw, M. R.; Thirumalai, D. *J. Chem. Phys.* **1990**, *93*, 3460. Laria, D.; Wu, D.; Chandler, D. *J. Chem. Phys.* **1991**, *95*, 4444.
- (21) Zhu, J.; Cukier, R. I. *J. Chem. Phys.* **1993**, *99*, 1288.
- (22) Zhu, J.; Cukier, R. I. *J. Chem. Phys.* **1993**, *99*, 5384.
- (23) This observation should be regarded with some caution since our simulated system is relatively small (100 solvent particles in a box of linear size 40 au). Also note that it is possible that at considerably larger values of μ the solvent structure will change; e.g., crystallization may occur, which may cause a qualitative change in the electronic wave function. We did not explore this possibility in the present work.
- (24) We do not expect that the solvent intramolecular vibrations strongly influence the level and the gap fluctuations. During the adiabatic motion these modes essentially remain in their ground state at the temperature considered. Nevertheless, these modes affect the nonadiabatic transition (see section 5).
- (25) Mosyak, A.; Nitzan, A. In *Reaction Dynamics in Clusters and Condensed Phases*; Pullman, B., Jortner, J., Levine, R. D., Eds.; Kluwer: Amsterdam, 1994; p 557.

JP960961T